Eur. Phys. J. C 22, 647–654 (2002)
Digital Object Identifier (DOI) 10.1007/s100520100839

THE EUROPEAN PHYSICAL JOURNAL C

Diffractive dissociation and saturation scale from non-linear evolution in high energy DIS

E. Levin[1,2,a], M. Lublinsky[3,4,b]

[1] HEP Department, School of Physics and Astronomy, Raymond and Beverly Sackler Faculty of Exact Science, Tel Aviv University, Tel Aviv 69978, Israel
[2] DESY Theory Group, 22602, Hamburg, Germany
[3] Department of Physics, Technion – Israel Institute of Technology, Haifa 32000, Israel
[4] II. Institut für Theoretische Physik, Universität Hamburg, Luruper Chaussee 149, 22761 Hamburg, Germany

Received: 29 August 2001 / Revised version: 25 October 2001 /
Published online: 14 December 2001 –

Abstract. This paper presents the first numerical solution to the non-linear evolution equation for diffractive dissociation processes in deep inelastic scattering. It is shown that the solution depends on one scaling variable $\tau = Q^2/Q_{\rm s}^{\rm D2}(x,x_0)$, where $Q_{\rm s}^{\rm D}(x,x_0)$ is the saturation scale for the diffraction processes. The dependence of the saturation scale $Q_{\rm s}^{\rm D}(x,x_0)$ on both x and x_0 is investigated, ($Y_0 = \ln(1/x_0)$ is the minimal rapidity gap for the diffraction process). The x-dependence of $Q_{\rm s}^{\rm D}$ turns out to be the same as the one of the saturation scale in the total inclusive DIS cross section. In our calculations $Q_{\rm s}^{\rm D}(x,x_0)$ reveals only a mild dependence on x_0. The scaling is shown to hold for $x \ll x_0$ but is violated at $x \sim x_0$.

1 Introduction

Diffractive inclusive production in deep inelastic scattering (DIS) at high energy has become an area of particular interest to experts, since it provides a deeper insight into the dynamics of QCD in the kinematic region where the density of partons is expected to be high (see [1] and the references therein).

Inclusive diffraction in DIS offers an opportunity to probe the transition region between "soft" and "hard" interactions giving natural estimates for the value of the shadowing corrections in DIS, namely $\Delta F_2 = F_2 - F_2^{\rm DGLAP} = F_{\rm D}$ [1] as was firstly shown in [3] on the basis of the AGK cutting rules [4]. A more detailed approach started with the Kovchegov–McLerran [5] formula which expresses the ratio of the diffraction cross section ($\sigma_{\rm diff}$) to the total cross section ($\sigma_{\rm tot}$) in DIS initiated by the quark–antiquark pair produced in $\gamma^* \to q + \bar{q}$ decay of the virtual photon. This formula reads

$$R = \frac{\sigma_{\rm diff}}{\sigma_{\rm tot}} = \frac{\int {\rm d}^2b \int {\rm d}z \int {\rm d}^2r_\perp P^{\gamma^*}(z,r_\perp;Q^2) N^2(r_\perp,x;b)}{2\int {\rm d}^2b \int {\rm d}z \int {\rm d}^2r_\perp P^{\gamma^*}(z,r_\perp;Q^2) N(r_\perp,x;b)}, \quad (1.1)$$

where $N(r_\perp,x;b)$ is the imaginary part of the elastic dipole–target amplitude for a dipole of the size $r_\perp$ scattered at fixed Bjorken variable $x = Q^2/W^2$ (Q^2 is the photon virtuality and W is its energy in the target rest frame) and at fixed impact b. $P^{\gamma^*}(z,r_\perp;Q^2)$ is the probability to find a quark–antiquark pair with size $r_\perp$ inside the virtual photon [6,7]:

$$\begin{aligned} P^{\gamma^*}(z,r_\perp;Q^2) &= \frac{\alpha_{\rm em}N_c}{2\pi^2}\sum_f Z_f^2 \sum_{\lambda_1,\lambda_2}\left\{|\Psi_{\rm T}|^2 + |\Psi_{\rm L}|^2\right\} \\ &= \frac{\alpha_{\rm em}N_c}{2\pi^2}\sum_f Z_f^2\Big\{(z^2+(1-z)^2)a^2K_1^2(ar_\perp) \\ &\quad + 4Q^2z^2(1-z)^2K_0^2(ar_\perp)\Big\}, \end{aligned} \quad (1.2)$$

where in the quark massless limit $a^2 = z(1-z)Q^2$. The functions $\Psi_{\rm T,L}$ stand for transverse and longitudinal polarized photon wave functions. Equation (1.1) is important since it provides a relation between the dipole–target elastic amplitude and the cross section of the diffraction dissociation. A non-linear evolution equation was derived for the former [8–14]. This equation has been studied both analytically [14,15] and numerically [13,16–18].

The formula (1.1) fails to describe correctly the experimental data on the diffraction production. Moreover, inclusion of an extra gluon emission in the initial virtual photon wave function is still insufficient to reproduce the data [19–22]. Nevertheless, (1.1) can be viewed rather as the initial condition to a more complicated equation.

The non-linear equation for the diffraction dissociation processes can be written for the amplitude $N^{\rm D}$ which has the following meaning [23].

[a] e-mail: leving@post.tau.ac.il
[b] e-mail: mal@techunix.technion.ac.il

[1] $F_{\rm D}$ is the diffractive structure function introduced in [2]

We introduce the cross section for diffraction production with the rapidity gap larger than given $Y_0 \equiv \ln(1/x_0)$:

$$\sigma_{\rm diff}(x,x_0,Q^2) = \int {\rm d}^2 r_\perp \int {\rm d}z P^{\gamma^*}(z,r_\perp;Q^2)\sigma^{\rm diff}_{\rm dipole}(r_\perp,x,x_0), \tag{1.3}$$

and

$$\sigma^{\rm diff}_{\rm dipole}(r_\perp,x,x_0) = \int {\rm d}^2 b N^{\rm D}(r_\perp,x,x_0;b). \tag{1.4}$$

The function $N^{\rm D}$ is the amplitude of the diffraction production induced by the dipole with size $r_\perp$ with rapidity gap larger than given (Y_0). Note that the minimal rapidity gap Y_0 can be kinematically related to the maximal diffractively produced mass: $x_0 = (Q^2+M^2)/W^2$.

The non-linear evolution equation for $N^{\rm D}$ was derived in [23] and recently rederived in [21]:

$$\begin{aligned} &N^{\rm D}(\boldsymbol{x_{01}},Y,Y_0;b) \\ &= N^2(\boldsymbol{x_{01}},Y_0;b){\rm e}^{-(4C_F\alpha_{\rm S}/\pi)\ln(\boldsymbol{x_{01}}/\rho)(Y-Y_0)} \\ &+\frac{C_F\alpha_{\rm S}}{\pi^2}\int_{Y_0}^{Y}{\rm d}y{\rm e}^{-(4C_F\alpha_{\rm S}/\pi)\ln(\boldsymbol{x_{01}}/\rho)(Y-y)} \\ &\times\int_\rho {\rm d}^2\boldsymbol{x_2}\frac{\boldsymbol{x_{01}^2}}{\boldsymbol{x_{02}^2}\boldsymbol{x_{12}^2}}\Bigg[2N^{\rm D}\left(\boldsymbol{x_{02}},y,Y_0;\boldsymbol{b}-\frac{1}{2}\boldsymbol{x}_{12}\right) \\ &+N^{\rm D}\left(\boldsymbol{x_{02}},y,Y_0;\boldsymbol{b}-\frac{1}{2}\boldsymbol{x}_{12}\right) \\ &\times N^{\rm D}\left(\boldsymbol{x_{12}},y,Y_0;\boldsymbol{b}-\frac{1}{2}\boldsymbol{x}_{02}\right) \\ &-4N^{\rm D}\left(\boldsymbol{x_{02}},y,Y_0;\boldsymbol{b}-\frac{1}{2}\boldsymbol{x}_{12}\right)N\left(\boldsymbol{x_{12}},y;\boldsymbol{b}-\frac{1}{2}\boldsymbol{x}_{02}\right) \\ &+2N\left(\boldsymbol{x_{02}},y;\boldsymbol{b}-\frac{1}{2}\boldsymbol{x}_{12}\right)N\left(\boldsymbol{x_{12}},y;\boldsymbol{b}-\frac{1}{2}\boldsymbol{x}_{02}\right)\Bigg]. \end{aligned} \tag{1.5}$$

Equation (1.5) describes a diffraction process initiated by the dipole of the size $\boldsymbol{x_{01}}$ which subsequently dissociates to two dipoles with sizes $\boldsymbol{x_{02}}$ and $\boldsymbol{x_{12}}$. The rapidity Y is defined as $Y = \ln(1/x)$ [2].

The evolution (1.5) is subject to the initial conditions at $x = x_0$:

$$N^{\rm D}(r_\perp,x_0,x_0;b) = N^2(r_\perp,x_0;b). \tag{1.6}$$

Namely, at an energy equal to the energy gap, diffraction is purely given by the elastic scattering as was stated in (1.1).

Since at high energies color dipoles are correct degrees of freedom [10] we can write the unitarity constraint

$$2N = N^{\rm D} + F, \tag{1.7}$$

where the function F denotes contributions of all the inelastic processes. An important observation is that F satisfies the same equation as N [11,12] but with shifted initial conditions [23]:

$$F_{\rm ini} = N_{\rm ini} - N^2_{\rm ini}. \tag{1.8}$$

Another interesting quantity to study is the cross section of a diffractive dissociation process with a fixed gap or equivalently to a fixed mass:

$$\Re \equiv -\partial N^{\rm D}/\partial Y_0. \tag{1.9}$$

The function $\Re$ was introduced in [23]. The authors of this paper proposed a model in which $\Re$ was shown to possess a maximum when varying Y_0 at fixed Y. Physically this maximum means that at given Y there is a preferable mass for the production. Below we will argue that the appearance of the maximum is related to the scaling phenomena to be displayed by the function $N^{\rm D}$.

The present paper is entirely devoted to the numerical solution of (1.5). Various properties of the solutions $N^{\rm D}$ are investigated while our final goal computation of the diffraction cross section is published separately [24]. In Sect. 2 the solution of (1.5) is presented. Section 3 deals with the determination of the diffractive saturation scale. Scaling phenomena are discussed in Sect. 4. We draw conclusions in Sect. 5.

2 Solution of the non-linear equation

In this section we report on the numerical solution of (1.5). The method of iterations proposed in [16] is applied. The constant value for the strong coupling constant $\alpha_{\rm S} = 0.25$ is always used. The solutions are computed for $4\times10^{-5} \le x_0 \le 10^{-2}$ and within the kinematic region $10^{-7} \le x \le x_0$ and distances up to a few Fermi.

The function $N^{\rm D}$ is formally a function of four variables: the energy gap x_0, the Bjorken variable x, the transverse distance $r_\perp$, and the impact parameter b. We assume the impact parameter b to be much larger than a typical dipole size: $r_\perp \ll b$. Within this assumption the b-dependence is parametric only because the evolution kernel does not depend on b. However, the problem is still complicated and requires a very long numerical run. In order to simplify the problem we will proceed similarly to the treatment of the b-dependence of the function N [16]. In that paper we assumed the function N to preserve the very same b-dependence as introduced in the initial conditions:

$$N(r_\perp,x;b) = \left(1-{\rm e}^{-\kappa(x,r_\perp)S(b)}\right), \tag{2.10}$$

with $S(b)$ being a dipole profile function inside the target (In the present work $S(b) = \exp(-b^2/R^2)$ with $R^2 = 10\,{\rm GeV}^{-2}$.) and the function κ being related to the "$b = 0$" solution $\tilde{N}(r_\perp,x)$:

$$\kappa(x,r_\perp) = -\ln(1-\tilde{N}(r_\perp,x)). \tag{2.11}$$

[2] Note that in (1.5) and below we freely interchange between variables x (x_0) and $Y = \ln 1/x$ ($Y_0 = \ln 1/x_0$) as formal arguments of the functions N and $N^{\rm D}$. We hope this carelessness does not cause any confusion to the reader

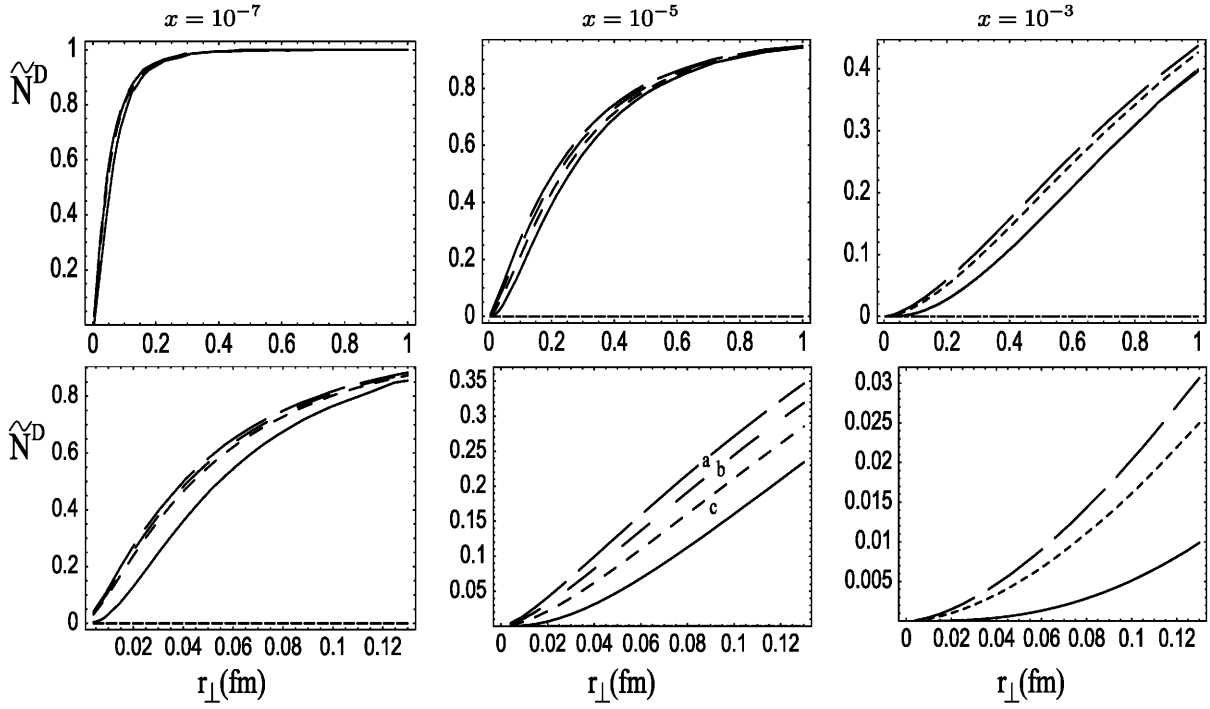

Fig. 1. The function $\tilde{N}^{\rm D}$ plotted versus the dipole transverse size. The curves correspond to different values of x_0: (a) $x_0 = 10^{-2}$; (b) $x_0 = 10^{-3}$; (c) $x_0 = 10^{-4}$. The solid line is $\tilde{N}^2$

$\tilde{N}(r_\perp, x)$ represents a solution of the very same non-linear equation (see [11,12]) but with no dependence on the third variable. The initial conditions for the function $\tilde{N}(r_\perp, x)$ are taken at $b = 0$. For the case of the proton target [16] the ansatz in the form (2.10) was shown to be a quite good approximation of the exact b-dependence of the solution to the non-linear equation for $N(r_\perp, x; b)$. In [17] we investigated the ansatz (2.10) for the gold target and again found it to be a very good approximation at least for impact parameters smaller than the target radius.

In order to be consistent with the initial conditions (1.6) we assume the following b-dependence of $N^{\rm D}$:

$$N^{\rm D}(r_\perp, x, x_0; b) = \left(1 - {\rm e}^{-\kappa^{\rm D}(x, x_0, r_\perp) S(b)}\right)^2, \qquad (2.12)$$

with

$$\kappa^{\rm D}(x, x_0, r_\perp) = -\ln\left(1 - \sqrt{\tilde{N}^{\rm D}(r_\perp, x, x_0)}\right). \qquad (2.13)$$

$\tilde{N}^{\rm D}(r_\perp, x, x_0)$ represents a solution of (1.5) but with no dependence on the fourth variable. The initial conditions for the function $\tilde{N}^{\rm D}(r_\perp, x, x_0)$ are set at $b = 0$ and $\kappa^{\rm D}(x_0, x_0, r_\perp) = \kappa(x_0, r_\perp)$. Since in the present paper we do not intend to compute cross sections for which we would need to perform the b integration, the accuracy of the ansatz (2.12) will not be investigated here.

For each initial value of x_0 the function $\tilde{N}^{\rm D}(r_\perp, x, x_0)$ is obtained after about ten iterations. Figure 1 shows the solutions $\tilde{N}^{\rm D}$ as a function of the transverse dipole size for various values of x_0 and x. The amplitude for the elastic scattering $\tilde{N}^2$ [16] is plotted in the same graph. The obtained numerical inequality $\tilde{N}^2 \leq \tilde{N}^{\rm D} \leq \tilde{N}$ is in perfect agreement with the physical expectations for the diffractive dissociation cross section to be larger than the elastic cross section. Another consistency check is the saturation of the function $\tilde{N}^{\rm D}$ which is a consequence of the unitarity bound. In the black disk limit diffractive dissociation is half of the total cross section.

It is worth to investigate the dependence of the solutions obtained on the gap variable x_0. To reach this goal we plot the function $N^{\rm D}$ as a function of the gap Y_0 for various transverse dipole sizes and at fixed $Y = 10$ (Fig. 2). At small sizes the solution depends strongly on x_0 though as we approach the saturation region this dependence dies out.

It was stated in the Introduction that the function $N^{\rm D}$ equals $2N - F$, where both functions N and F are solutions of the same non-linear equation [11,12]. Thus it is natural to compute $2N - F$ solving the non-linear evolution equation [11,12] with appropriate initial conditions. A comparison with $N^{\rm D}$ from (1.5) would be an ultimate test for the correctness of the numerical procedures. Such a test was successfully performed and we found an absolute agreement (relative error less than 1%) between both computations.

3 Saturation scale

Determination of the diffractive saturation scale $Q_{\rm s}^{\rm D}(x, x_0)$ from the solution $\tilde{N}^{\rm D}$ is subject of this section. Unfortunately, no exact mathematical definition of the saturation

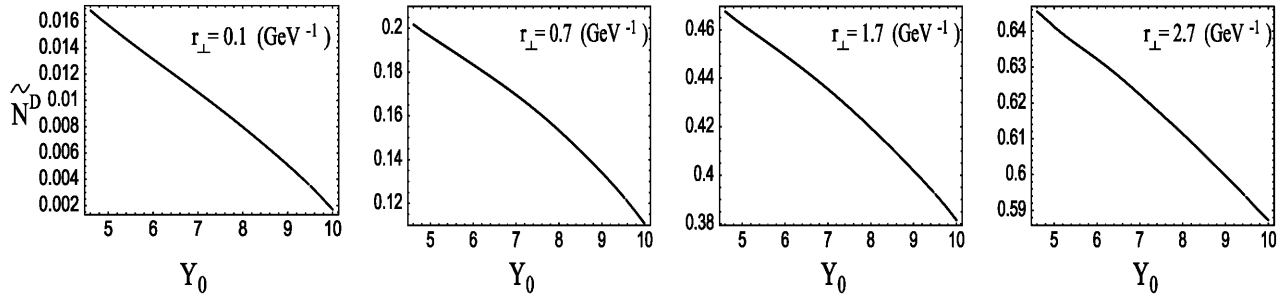

Fig. 2. The function $\tilde{N}^{\rm D}$ plotted versus the gap Y_0 at fixed rapidity $Y = 10$

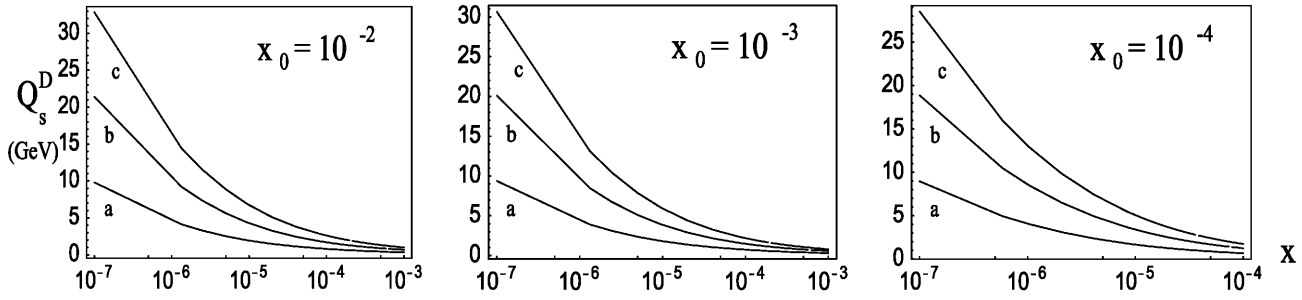

Fig. 3. The saturation scale $Q_{\rm s}^{\rm D}$ plotted versus x. The three curves correspond to the definitions (3.14) (lowest curve), (3.15) (middle curve), and (3.16) (upper curve)

scale is known so far. In [16,25] several definitions of the saturation scale $Q_{\rm s}(x)$ were proposed which related the saturation scale to the shape of the function $\tilde{N}$. It is important to stress that it is not clear a priori whether $Q_{\rm s}^{\rm D}$ should coincide with $Q_{\rm s}$ or not. We will proceed here in the same spirit as in [25]. Namely, we propose several definitions of the saturation scale while the variety of the obtained results will indicate the uncertainty in the definitions.

For a step-like function it is natural to define the saturation scale as the position where it reaches half of the maximum:

(1) Definition (a):

$$\tilde{N}^{\rm D}(R_{\rm s}^{\rm D}, x, x_0) = 1/2, \quad Q_{\rm s}^{\rm D} \equiv 2/R_{\rm s}^{\rm D}. \tag{3.14}$$

The equality between the saturation radius $R_{\rm s}^{\rm D}$ and the saturation scale $Q_{\rm s}^{\rm D}$ is motivated by the double logarithmic approximation. Though this approximation is formally not justified, we still believe it to yield reliable estimates provided $Q_{\rm s}^{\rm D}$ is large enough. The definition (3.14) is analogous to the one proposed in [16] $N(2/Q_{\rm s}, x) = 1/2$. If we recall that $N^{\rm D} = N^2$ at $x = x_0$ and postulate $Q_{\rm s}^{\rm D}(x_0, x_0) = Q_{\rm s}(x_0)$, then consistency requires

(2) Definition (b):

$$\tilde{N}^{\rm D}(2/Q_{\rm s}^{\rm D}, x, x_0) = 1/4. \tag{3.15}$$

An alternative definition of the saturation scale could be one motivated by the Glauber–Mueller formula:

(3) Definition (c):

$$\kappa^{\rm D}(2/Q_{\rm s}^{\rm D}, x, x_0) = 1/2. \tag{3.16}$$

The saturation scales deduced through the above definitions are depicted in Fig. 3. For given x_0 the observed hierarchy between the saturation scales obtained is an obvious consequence of the definitions (3.14), (3.15), (3.16) and the shape of the function $\tilde{N}^{\rm D}$ (Fig. 1). Note that the saturation scale is almost x_0-independent.

It is important to learn about the x-dependence of the saturation scale. To reach this goal, we assume the following parameterization:

$$Q_{\rm s}^{\rm D}(x, x_0) = Q_{\rm s0}^{\rm D} x^{-\lambda} x_0^{\beta}. \tag{3.17}$$

In fact, the parameterization (3.17) is a good approximation for the values of the saturation scales obtained with

$$\lambda = 0.385 \pm 0.015 \quad \text{and } \beta = 0.045 \pm 0.025.$$

Within the errors these powers coincide for all the saturation scale definitions (3.14), (3.15), (3.16). The small value for the power β is a numeric indication of the very weak x_0-dependence of the saturation scale. Its large relative error results on one hand from numerical limitations and on the other hand, this error signals a more complicated x_0-dependence than is given in (3.17).

It is important to stress that the obtained power λ coincides with the corresponding power of the saturation scale $Q_{\rm s}$ [25].

4 Scaling phenomena

In [25] the function $\tilde{N}$ was shown to display the scaling phenomenon. We present here a similar analysis for the function $\tilde{N}^{\rm D}$. In the saturation region the scaling implies

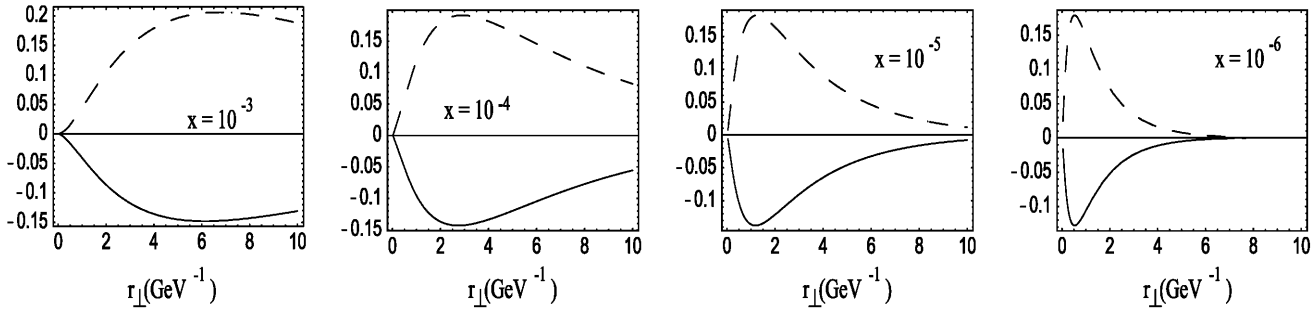

Fig. 4. The derivative functions $N_r^{\rm D}$ (dashed line) and $N_y^{\rm D}$ (solid line) as functions of the distance at fixed $x_0 = 10^{-2}$

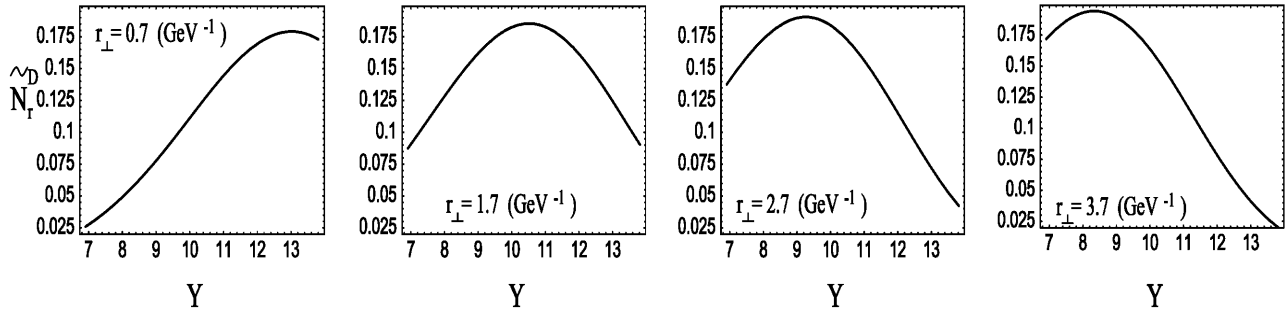

Fig. 5. The derivative function $N_r^{\rm D}$ as a function of the rapidity Y at $x_0 = 10^{-2}$

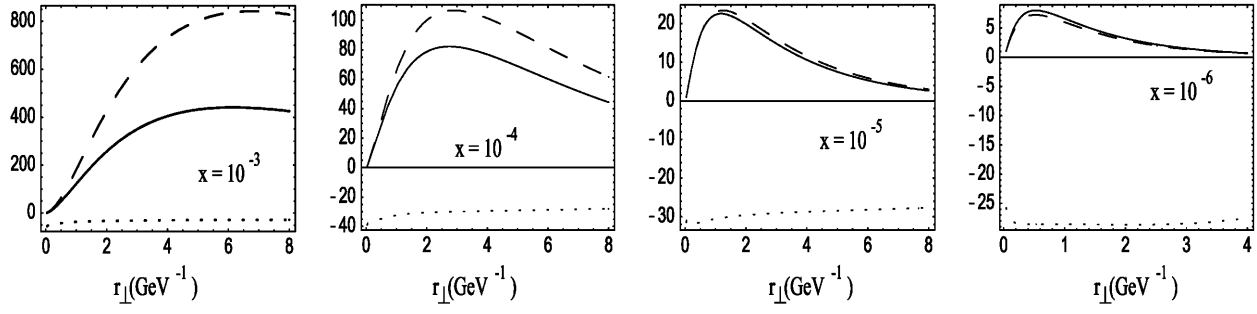

Fig. 6. The scaling as a function of the distance at fixed $x_0 = 10^{-2}$. The positive curves are $N_r^{\rm D}/N_{r\min}^{\rm D}$ (dashed line) and $N_y^{\rm D}/N_{y\min}^{\rm D}$ (solid line). The dotted line is $40 \times R_a^{\rm D}$

the amplitude to be a function of only one variable $\tau = (r_\perp \cdot Q_{\rm s}^{\rm D}(x, x_0))^2$:

$$\tilde{N}^{\rm D}(r_\perp, x, x_0) = \tilde{N}^{\rm D}(\tau). \tag{4.18}$$

Let us define the following derivative functions assuming the scaling behavior (4.18):

$$N_y^{\rm D}(r_\perp, x, x_0) \equiv -\frac{\partial \tilde{N}^{\rm D}}{\partial Y} = \frac{{\rm d}\tilde{N}^{\rm D}}{{\rm d}\tau}\tau\frac{\partial \ln(Q_{\rm s}^{\rm D})^2}{\partial \ln x}, \tag{4.19}$$

$$N_r^{\rm D}(r_\perp, x, x_0) \equiv r_\perp^2\frac{\partial \tilde{N}^{\rm D}}{\partial r_\perp^2} = \frac{{\rm d}\tilde{N}^{\rm D}}{{\rm d}\tau}\tau, \tag{4.20}$$

$$\Re(r_\perp, x, x_0) \equiv -\frac{\partial \tilde{N}^{\rm D}}{\partial Y_0} = \frac{{\rm d}\tilde{N}^{\rm D}}{{\rm d}\tau}\tau\frac{\partial \ln(Q_{\rm s}^{\rm D})^2}{\partial \ln x_0}. \tag{4.21}$$

If the scaling behavior (4.18) indeed occurs, then both the ratios $N_y^{\rm D}/N_r^{\rm D}$ and $\Re/N_r^{\rm D}$ are $r_\perp$-independent functions. Let us first consider scaling with respect to x. Figure 4 presents the derivatives $N_y^{\rm D}$ and $N_r^{\rm D}$ as functions of the distance $r_\perp$ at fixed $x_0 = 10^{-2}$. Both functions $N_y^{\rm D}$ and $N_r^{\rm D}$ have extrema placed at the same distance depending on x. This is a consequence of the scaling behavior (4.18), and (4.19) and (4.20). The extrema occur at certain $\tau_{\max}$, such that $\tilde{N}^{D\prime}(\tau_{\max}) = -\tau_{\max}\tilde{N}^{D\prime\prime}(\tau_{\max})$. In Fig. 4, $\tau_{\max}$ is approached by varying $r_\perp$ at fixed x. Alternatively it can be reached by varying x at fixed $r_\perp$ (Fig. 5).

Consider now the ratio function $R_a^{\rm D}$:

$$R_a^{\rm D}(r_\perp, x, x_0) \equiv \frac{N_y^{\rm D}}{N_r^{\rm D}} = \frac{\partial \ln(Q_{\rm s}^{\rm D})^2}{\partial \ln x}. \tag{4.22}$$

If the scaling phenomenon occurs the function $R_a^{\rm D}$ is expected to be $r_\perp$-independent. We study the scaling within the distance interval $0.04\,{\rm GeV}^{-1} \le r_\perp \le 10\,{\rm GeV}^{-1}$ that corresponds to $0.25\,{\rm GeV}^2 \le Q^2 \le 2.5\times10^3\,{\rm GeV}^2$. Figure 6 presents the results on the scaling. The three lines correspond to functions $N_r^{\rm D}$ and $N_y^{\rm D}$ divided by their minimal

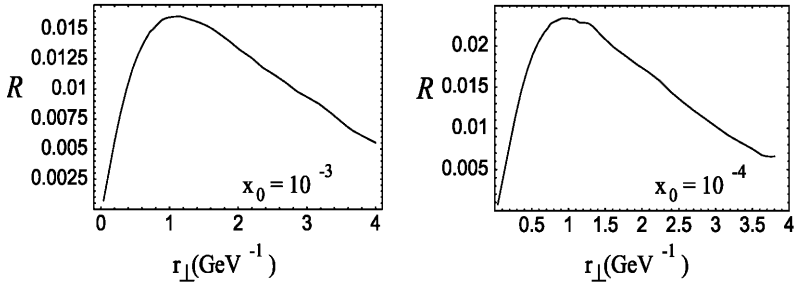

Fig. 7. The function $\Re$ versus distance at fixed $Y = 10$

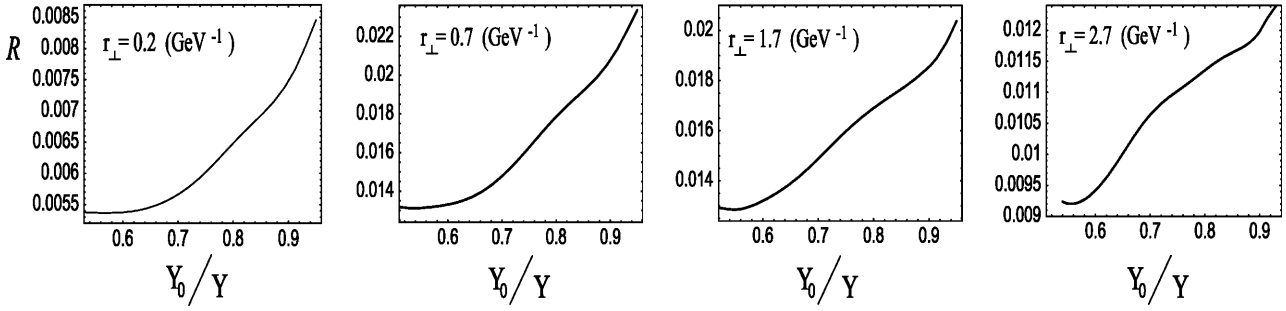

Fig. 8. The function $\Re$ as a function of the ratio Y_0/Y at fixed $Y = 10$

values within the interval, and the function $R_a^{\rm D}$ multiplied by the factor 40 to be seen on the scale.

The function $R_a^{\rm D}$ is clearly observed to be a very slowly varying function of $r_\perp$ for all values of x and $r_\perp$. Though at fixed x the function $R_a^{\rm D}$ cannot be claimed to be an exact constant, its variations with $r_\perp$ are very much suppressed compared to the variations of the functions $N_r^{\rm D}$ and $N_y^{\rm D}$. For example, at $x = 10^{-5}$ within the given interval the function $R_a^{\rm D}$ changes by maximally 20%, while within the very same interval both functions $N_r^{\rm D}$ and $N_y^{\rm D}$ change by several times. Then the relative fluctuation is much less than 10%, which confirms the scaling. The phenomenon holds with a few percent accuracy and it improves at smaller $x \simeq 10^{-7}$ and in the deep saturation region. However to observe this scaling behavior in these regions is numerically more problematic since both derivatives $N_r^{\rm D}$ and $N_y^{\rm D}$ tend to zero.

The above analysis was performed for the fixed value $x_0 = 10^{-2}$. Within the errors the function $R_a^{\rm D} \simeq -0.75 \pm 0.08$, constant independent on both $r_\perp$ and x. Moreover, if we repeat the same program but for different values of x_0, we discover quite similar scaling phenomena with $R_a^{\rm D}$ being numerically independent on x_0 as well. This observation implies

$$Q_{\rm s}^{\rm D}(x, x_0) = Q_{\rm s0}^{\rm D}(x_0) x^{-\lambda}, \quad \lambda = 0.37 \pm 0.04. \qquad (4.23)$$

Note that the value obtained for λ is in agreement with the one determined in the previous section.

Let us now study the scaling behavior with respect to the variable x_0. To this aim we investigate the function $\Re$ which is related to the x_0-dependence of the saturation scale $Q_{\rm s0}^{\rm D}$. Assuming $Q_{\rm s0}^{\rm D} \sim x_0^\beta$ we predict $\Re$ to have a maximum at $\tau = \tau_{\rm min}$. Figure 7 displays the function $\Re$ as a function of the distance at fixed $x = 4.54 \cdot 10^{-5}$ ($Y = 10$). In complete agreement with the scaling assumption (4.21) the function $\Re$ possesses a maximum with respect to $r_\perp$ variations. The heights of the maxima are proportional to β. Since $\tau \tilde{N}^{D\prime}(\tau)|_{\tau=\tau_{\rm max}} \simeq 0.2$, β can be estimated to be approximately 0.05 ± 0.02, which agrees with the value deduced earlier.

We can learn more about the scaling if we consider the function $\Re$ as a function of x_0 or the energy gap Y_0. In [23] a model was built in which the function $\Re$ had a maximum with respect to the Y_0 variation at fixed Y. We know now that this maximum is a consequence of the scaling phenomena. The dependence of $\Re$ on Y_0 at $Y = 10$ is plotted in Fig. 8.

No maxima are observed on the plots of Fig. 8. In fact this is a sign of the scaling violation so far avoided by the discussion. The scaling with respect to x_0 is not exact at $Y_0 \simeq Y$. Due to its smallness ($\Re \propto \beta$) the function $\Re$ is most sensitive to small deviations from the scaling behavior:

$$\tilde{N}^{\rm D}(r_\perp, x, x_0) = \tilde{N}^{\rm D}_{\rm scaling}(\tau) + \delta\tilde{N}^{\rm D}(r_\perp, x, x_0). \qquad (4.24)$$

In the kinematic region of the investigation variations of the function $\delta\tilde{N}^{\rm D}$ with respect to $r_\perp$ and x are small compared to variations of $\tilde{N}^{\rm D}_{\rm scaling}$. On the contrary, the derivative of $\delta N^{\rm D}$ with respect to Y_0 is of the same order as the derivative of $\tilde{N}^{\rm D}_{\rm scaling}$. This is the origin of the large errors of β and the x_0 scaling violation at $x_0 \simeq x$.

In order to complete the analysis of the scaling we plot the function $\tilde{N}^{\rm D}$ as a function of τ at different values of x and x_0 (Fig. 9). The overall normalization of the saturation scale cannot be deduced from the scaling analysis only. We choose the following normalization: $Q_{\rm s}^{\rm D}(x = 10^{-7}, x_0 = 10^{-2}) = 20\,{\rm GeV}$. In Fig. 9 the cluster of the curves correspond to the $(x = 10^{-7}, x_0 = 10^{-2}), (x = 10^{-5}, x_0 = 10^{-2}), (x = 10^{-3}, x_0 = 10^{-2}), (x = 10^{-7}, x_0 = 10^{-3}), (x = 10^{-7}, x_0 = 10^{-4})$, and $(x = 10^{-5}, x_0 = 10^{-3})$

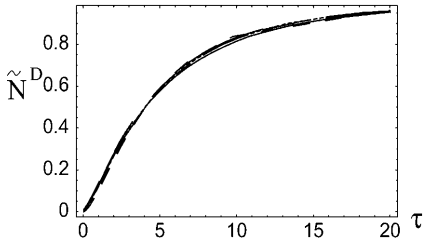

Fig. 9. The function $\tilde{N}^{\rm D}$ plotted versus τ for various values of x and x_0: $x = 10^{-7}, x_0 = 10^{-2}$; $x = 10^{-5}, x_0 = 10^{-2}$; $x = 10^{-3}, x_0 = 10^{-2}$; $x = 10^{-7}, x_0 = 10^{-3}$; $x = 10^{-7}, x_0 = 10^{-4}$; and $x = 10^{-5}, x_0 = 10^{-3}$

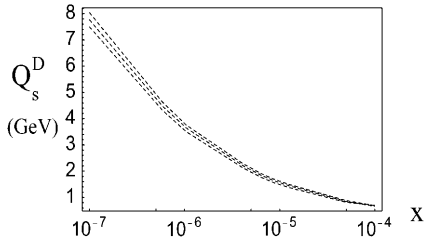

Fig. 10. The saturation scale deduced from (4.25). The different curves correspond to $x_0 = 10^{-2}$ (the upper curve), 10^{-3} (middle curve) and $x_0 = 10^{-4}$ (the lowest curve)

curves. The approximate independence of the curves on the values of x and x_0 is another and probably most illustrative manifestation of the scaling phenomena.

Finally we propose yet another definition of the saturation scale based on the above presented scaling analysis. It is natural to define the saturation radius at the position where $\tau\tilde{N}'(\tau)$ has a maximum, namely at $\tau_{\max}$:

(4) Definition (d):

$$\left(\frac{\partial(\tau\tilde{N}'(\tau))}{\partial r_\perp^2}\right)_{r_\perp^2=4/(Q_{\rm s}^D)^2} = 0. \qquad (4.25)$$

The saturation scale obtained from (4.25) is depicted in Fig. 10. Note again the weak dependence on the value of x_0.

5 Conclusions

The non-linear evolution equation (1.5) is solved numerically by the method of iterations. The solutions obtained are in agreement with the unitarity constraints: the diffraction dissociation is larger than just the elastic scattering but smaller than or equal to half of the total.

The diffractive saturation scale $Q_{\rm s}^{\rm D}$ is estimated from the solutions of (1.5) based on four different definitions of the saturation scale. Though there exists a significant uncertainty in the absolute values of the scale its x-dependence is found to be the same as of the $Q_{\rm s}$-saturation scale deduced from the non-linear equation for $\tilde{N}$ [11,12]. In fact this result is quite natural. The dependence of the saturation scale on x is an entire property of the evolution equation and it should not depend on both initial conditions and the saturation scale definition. The saturation scale $Q_{\rm s}^{\rm D}$ is discovered to be almost independent on the minimal gap x_0.

Both saturation scales $Q_{\rm s}$ and $Q_{\rm s}^{\rm D}$ are proportional to $x^{-\lambda}$ with $\lambda \simeq 0.38$. This result is certainly very sensitive to the value of $\alpha_{\rm s}$ and it was obtained at fixed $\alpha_{\rm s} = 0.25$. The double logarithmic prediction of [15] is $\lambda = 2\alpha_{\rm s}N_c/\pi$, which for the given value of $\alpha_{\rm s}$ leads to $\lambda \simeq 0.5$. It is worth to investigate numerically the dependence of the power λ on $\alpha_{\rm s}$. To reach this goal we need to solve (1.5) at different values of $\alpha_{\rm s}$, which is our nearest future project.

The scaling phenomena with respect to all variables were studied in detail. The scaling with respect to x is well established. It holds with a few percent accuracy in the whole kinematic region investigated. The discovered scaling should manifest itself in the experiments on diffraction, and hence it would be interesting to search for it in the $F_2^{\rm D}(x,Q^2)/(Q^2S)$ experimental data (S stands for the target transverse area).

The numerically observed small scaling violation shows up when we consider the scaling with respect to x_0. This happens due to the weak sensitivity of the solutions to the variation of x_0. As a result, the variations of the solutions with respect to x_0 are of the same order as the scaling violation. The scaling sets in at $x \ll x_0$ but is violated at $x \sim x_0$.

The detailed analysis of the ratio between the total diffractive dissociation and the total DIS cross section is presented in a separate publication [24]. Our computations show that this ratio happens to be independent on the central mass energy in agreement with the experimental data [2]. This independence can be traced back to the scaling property displayed by the amplitudes N and $N^{\rm D}$ and to the fact that both saturation scales depend on x with the very same power λ.

Acknowledgements. The authors are very much indebted to Jochen Bartels, Krystoff Golec-Biernat and Yuri Kovchergov for numerous helpful discussions about diffraction production in DIS. We would like to thank Asher Gotsman, Uri Maor, Eran Naftali and Kirill Tuchin for many informative and encouraging discussions. We thank DESY theory group and Hamburg University Institute of theoretical physics for their hospitality and the creative atmosphere during several stages of this work. The research of E.L. was supported in part by the BSF grant # 9800276, by GIF grant # I- 620.-22.1411444 and by Israeli Science Foundation, founded by the Israeli Academy of Science and Humanities. The work of M.L. was partially supported by the Minerva Foundation and its financial help is gratefully acknowledged.

References

1. M. Wüsthoff, A.D. Martin, J. Phys. G **25**, R309 (1999)
2. H1 collaboration: T. Ahmed et al., Phys. Lett. B **348**, 681 (1995); ZEUS collaboration: J. Breitweg et al., Eur. Phys. J. C **6**, 43 (1999)
3. E. Levin, M. Wüsthoff, Phys. Rev. D **50**, 4306 (1994)

4. V.A. Abramovsky, V.N. Gribov, O.V. Kancheli, Yad. Fiz. **18**, 595 (1973) [Sov. J. Nucl. Phys. **18**, 308 (1973)]
5. Y.V. Kovchegov, L. McLerran, Phys. Rev. D **60**, 054025 (1999); Erratum ibid. D **62**, 019901 (1999)
6. A.H. Mueller, Nucl. Phys. B **335**, 115 (1990)
7. N.N. Nikolaev, B.G. Zakharov, Z. Phys. C **49** 607 (1991); Phys. Lett. B **260** 414 (1991); E. Levin, M. Wüsthoff, Phys. Rev. D **50**, 4306 (1994); E. Levin, A.D. Martin, M.G. Ryskin, T. Teubner, Z. Phys. C **74**, 671 (1997)
8. L.V. Gribov, E.M. Levin, M.G. Ryskin, Phys. Rep. **100**, 1 (1981)
9. A.H. Mueller, J. Qiu, Nucl. Phys. B **268**, 427 (1986)
10. A.H. Mueller, Nucl. Phys. B **415**, 373 (1994)
11. Ia. Balitsky, Nucl. Phys. B **463**, 99 (1996)
12. Yu. Kovchegov, Phys. Rev. D **60**, 034008 (2000)
13. M. Braun, Eur. Phys. J. C **16**, 337 (2000), hep-ph/0101070
14. E. Iancu, A. Leonidov, L. McLerran, hep-ph/0011241; E. Iancu, L. McLerran, Phys. Lett. B **510**, 145 (2001)
15. Yu. Kovchegov, Phys. Rev. D **61**, 074018 (2000); E. Levin, K. Tuchin, Nucl. Phys. B **573**, 833 (2000); hep-ph/01012175; Nucl. Phys. A **691**, 779 (2001)
16. M. Lublinsky, E. Gotsman, E. Levin, U. Maor, hep-ph/0102321, Nucl. Phys. A (in press)
17. E. Levin, M. Lublinsky, hep-ph/0104108, Nucl. Phys. A (in press)
18. N. Armesto, M. Braun, Eur. Phys. J. C **20**, 517 (2001)
19. E. Gotsman, E. Levin, M. Lublinsky, U. Maor, K. Tuchin, hep-ph/0007261, Nucl. Phys. A (in press)
20. B.Z. Kopeliovich, I.K. Potashnikova, B. Povh, E. Predazzi, Phys. Rev. D **63**, 054001 (2001)
21. A. Kovner, U.A. Wiedemann, hep-ph/0106240
22. Y.V. Kovchegov, hep-ph/0107256
23. Yu. Kovchegov, E. Levin, Nucl. Phys. B **577**, 221 (2000)
24. E. Levin, M. Lublinsky, hep-ph/0108265, DESY-01-124, Phys. Lett. B (in press)
25. M. Lublinsky, Eur. Phys. J. C **21**, 513 (2001)